J Sol-Gel Sci Technol (2015) 74:641–649
DOI 10.1007/s10971-015-3643-2

ORIGINAL PAPER

Development of universal pH sensors based on textiles

Xiao-Zhu Sun · Christopher Branford-White · Zhi-Wu Yu · Li-Min Zhu

Received: 9 November 2014 / Accepted: 22 January 2015 / Published online: 6 February 2015

Abstract We report that halochromic textiles are promising sensory system for measuring changes in pH. The system is easy to manage and process. In this study a universal pH sensitive textile was developed using a sol–gel method, which recorded pH by displaying unique color. The indicators incorporated in the sol system are different and are dependent on the substrate used. Samples demonstrated sufficient stability against leaching on account of the hybrid structure generated in the silicon matrix. Moreover, the interaction between the gel matrix and indicators depended on the charges and size of the guest molecules, and the tensile strength of cotton was enhanced by the gel film. The present research opens up new avenues to develop sensors based on textiles which have the potential to be employed in wider industrial applications.

Graphical Abstract

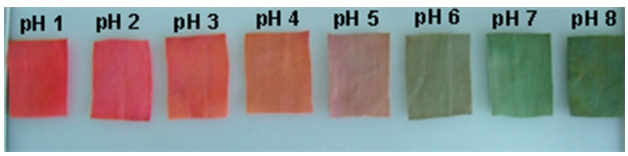

X.-Z. Sun · L.-M. Zhu (✉)
College of Chemistry Chemical Engineering and Biotechnology, Donghua University, Shanghai 201620, People's Republic of China
e-mail: lzhu@dhu.edu.cn

C. Branford-White
Faculty of Life Sciences and Computing, London Metropolitan University, London N7 8DB, UK

Z.-W. Yu
High Magnetic Field Laboratory, Hefei Institutes of Physical Science, Chinese Academy of Sciences, Hefei 230031, Anhui, People's Republic of China

Keywords Sol–gel · pH sensor · Smart textile · Halochromic

1 Introduction

Sol–gel technology is a relatively simple process which has been widely used in producing films, fibers, particles or composites. Materials include simple inorganic glass to complex organic–inorganic hybrid networks that can be prepared by the hydrolysis and condensation of precursors such as silicon alkoxides [1–3]. This provides a suitable matrix for the immobilization or encapsulation of guest molecules such as drugs, food materials and chemicals [4–7].The development of pH sensors through the entrapment of indicators in a sol–gel based matrix is of particular concern due to optical transparency, mechanic stability, configuration flexibility, proton permeability and low chemical reactivity [8–10]. Several studies have been undertaken to determine the influence of the synthetic route in the preparation and interactions between immobilized molecules and sol–gel glass [11–13]. Existing sol–gel prepared pH sensors were mainly applied on a rigid substrate like silicon wafer by spin coating. There is a potential to develop a textile-based flexible pH sensor with light weight, breathability a large coverage.

A series of technical textiles with various functionalities, including fiber protection, solvent repellency, electromagnetic property, bioactive layers, have been achieved by using of sol–gel coatings [14–17]. Dip and padding processes followed by a thermal treatment are commonly used in the textile industry so creating new surface properties to the textiles. Light absorption of textiles can also be changed by sol–gel systems. Similar to traditional dyeing process, textiles can be color stained by organic dyestuff

doped sols coating. This enhances the washing fastness and photostability [18]. Durable UV-blocking protection and stable photochemical properties have been used for textiles by embedding TiO_2 or light-sensitive dyestuffs into the sol matrices [19, 20].

To date studies on color-changing textiles have mainly dealt with thermochromism or photochromism systems that are temperature or light sensitive [21, 22]. Thus, use of halochromic textiles that respond to pH changes should be considered. These materials can be applied in various ways such as protective clothing to identify harmful/toxic vapor, wound dressing to monitor the recovery progress and filtration to assess water pH [23, 24]. However the main body of research relating to pH-sensitive textiles are carried out using conventional dyeing processes so potentially resulting in poor water fastness due to a lack of covalent linking and compatibility between the textile and pH-sensor [25]. Schueren et al. [26] covalently attached methyl red (MR) to sols through the epoxy group and as an outcome a durable halochromic complex was prepared. One indicator was used in the system so limiting the pH range and versatility of the system. Thus it would be of interest if a system could be developed that covered a wider range of pH using distinctive dyes covering the chromic spectrum.

In the present study, we report the treatment of cotton fabrics using a hybrid sol–gel, which incorporated four pH sensors. These were able to measure the pH value over a wide range. Halochromism properties and pH changes were characterized by reflectance spectroscopy, CIE color space, and infrared spectroscopy. Leaching characteristics, which often play a role in continuous operational use and long-term stability, were evaluated and assessed by solid NMR spectra, and the interaction between guest molecules and gel matrix was investigated as well. Tensile strength (TS) analyses were undertaken to examine the physical properties of cotton fabric.

2 Experimental

2.1 Materials

Methyl red, Phenol Red (PR), Bromocresol Green (BCG) and Bromothymol Blue (BTB) were purchased from the Sinopharm Chemical Reagent Co. Ltd. The sol–gel precursor glycidoxypropyltrimethoxysilane (GPTMS) and tetraethoxysilane (TEOS) were provided by the Tcishanghai Co. Ltd. Scoured and bleached cotton fabric were supplied by Dayao Textile. Hydrochloric acid (38 %) was used as a catalyst and all other chemicals and reagents were of analytical grade. Human smooth muscle cell lines were purchased from cell bank of Chinese Academy of Sciences.

2.2 Preparation

The precursor TEOS and GPTMS, silicon alkoxide was dissolved in a mixture of ethanol, water and HCl (1:1:8:50:8 $\times$ 10^{-3} molar ratio) and stirred for 4 h. The solution was mixed with pH-sensitive dye (MR, PR, BCG or BTB).

The ratio was 1:200 ($n_{precursor}$: n_{dye}) and controls lacking indicators were also prepared. When a combination of dyes was used, each of which were of the same amount. The sol solutions were prepared after another 1 h and then the cotton samples were impregnated with sol solutions and passed through a two-roll laboratory padder (Yuanmore Co. Ltd.) at a water pick-up rate of 80 % and this process was repeated. After drying at 60 °C for 15 min, fabrics were cured at 120 °C for 60 min in an electric laboratory oven. Conventional dyeing samples were prepared using the same process apart from the addition of the precursors.

The sol solutions with or without indicators were poured into Petri dishes, and dried at 60 °C for 6 h, cured at 120 °C for 1 h in an air circulation oven. Gel powders were prepared by grinding the matrix.

2.3 Methods

To assess the prepared halochromism both the sol–gel finished cotton or the sol solutions were added to a series of buffers ranging from pH 1–8. The pH 3–8 buffers was prepared using Na_2HPO_4 and citric acid, and pH 1–2 by diluting with HCl.

The morphology of the fabrics was analyzed by scanning electron microscopy (SEM; JSM-5600LV, JEOL, Japan) and samples were gold sputter-coated under argon prior to imaging.

UV–Vis spectra were recorded with Perkine-Elmer Lambda 35 spectrophotometer. For the absorption of sol solutions 1 cm matched quartz cells were used and the reflection measurements on sol–gel finished fabrics were taken with an integrated sphere (50 mm). The spectra was measured 400–800 nm with a data interval of 1 nm.

The color assessment was determined using a Datacolor 600 at $D65/10^0$ illuminant. The magnitude of the color difference was quantified by ΔE, with ΔL being the lightness difference, Δa^* and Δb^* the differences in redness and yellowness values.

$$\Delta E = \sqrt[2]{(\Delta L)^2 + (\Delta a^*)^2 + (\Delta b^*)^2}.$$

Fourier transformed infrared spectroscopy(FTIR) was conducted using a Nicolet-Nexus 670 FTIR spectrometer (Nicolet Instrument Corporation, Madison, USA) with the 500–4,000 cm^{-1} scanning range and a resolution of 2 cm^{-1}.

^{13}C NMR spectra of precursors were obtained in $CDCl_3$ with a Bruker Avance 400 spectrometer. ^{13}C and ^{29}Si solid state NMR of gel was recorded at frequencies of 75.5 MHz for CP/MAS NMR with referencing to an external standard, tetramethylsilane (TMS).

The leaching stability studies were conducted at 37 °C and 100 rpm in a thermostatic shaking incubator (Jintan Instrument Co. Ltd.) with 50 ml water and a 3 × 3 cm fabric. The water was changed after 24 h and the fabric impregnated from zero, 24 and 48 h were analyzed by K/S value, with ρ being the absorbance at the wavelength of maximum absorption.

$$K/S = \frac{(1-\rho)^2}{2\rho}.$$

Measurements were conducted in quadruplicate, and results reported as average values ± SD.

Tensile strength and elongation at break (E %) was determined according to ISO 13934-1:1994.

3 Results and discussion

3.1 Morphology

SEM images of the various samples are depicted in Fig. 1. It was noted that apart from a few grooves the surface of uncoated cotton is generally smooth. After treating with indicator free sol solution and adhesion of the coating resulted in a continuous film that included rough clusters and this was possibly due to a large number of nanoparticles being absorbed on to the surface. The entrapment of dyes adversely affected the formation of the film and these contained unevenly distributed cavities and agglomerated structures. This could be due to a poor compatibility between the dyes and the silica matrix [27].

3.2 Halochromic characteristics

Halochromism properties of the sol–gel finished cotton and the sol solutions were studied by placing samples in pHs varying from 1 to 8 (Fig. 2). Spectra measurements covered the red region (630–670 nm) orange–yellow (590–610 nm) and the green (540–560 nm) and the three maximum reflection are shown in Fig. 3 [28].

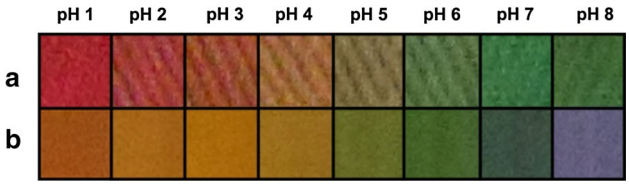

Fig. 2 Color transition between each pH in **a** sol–gel finished cotton with four indicators, **b** sol solutions containing four indicators

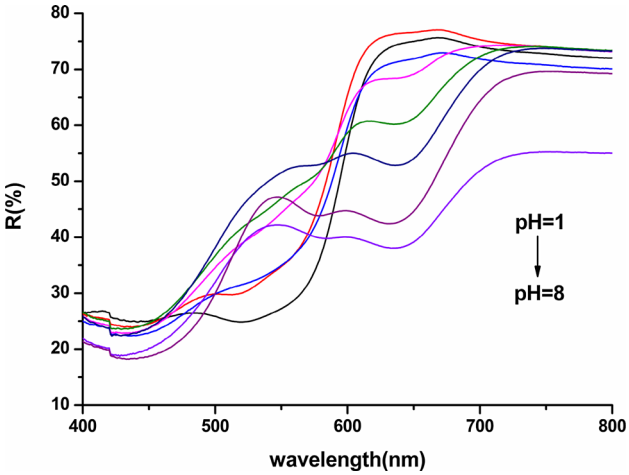

Fig. 3 Reflectance spectrum of sol–gel finished cotton with four indicators in different pH

At pH < 4 the reflectance above 600 nm exceeded 70 % and with no other prominent reflection region within the spectrum range. In this case the red spectra being dominant. As the pH rises (pH 4–5), the reflectance was reduced at around 640 nm and increased below 610 nm. Meanwhile, a new peak at 610 nm was observed and this was mainly a mixture of red and orange light. Along with increasing pH, a reduction in the 640 nm peak was evident which was replaced by a further peak at 540 nm and this reached a maximum reflectance at pH 7 and 8 that lies within the green region. Thus, the color of the textile was brought out by the combination of four indicators in different conformation for each pH level. As BTB, BCG and PR have the same tautomerism, FTIR spectra of MR and

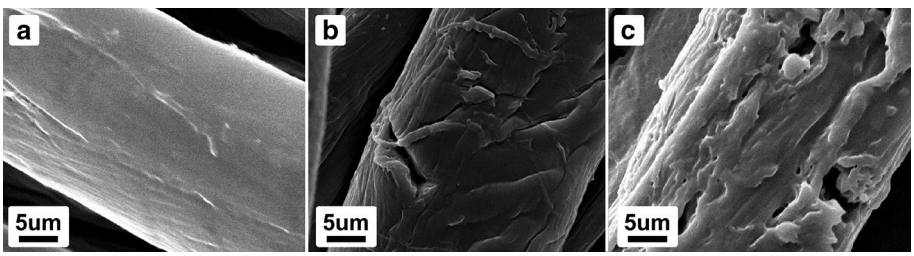

Fig. 1 SEM images of **a** untreated cotton, **b** sol–gel finished cotton without indicators, **c** sol–gel finished cotton with four indicators

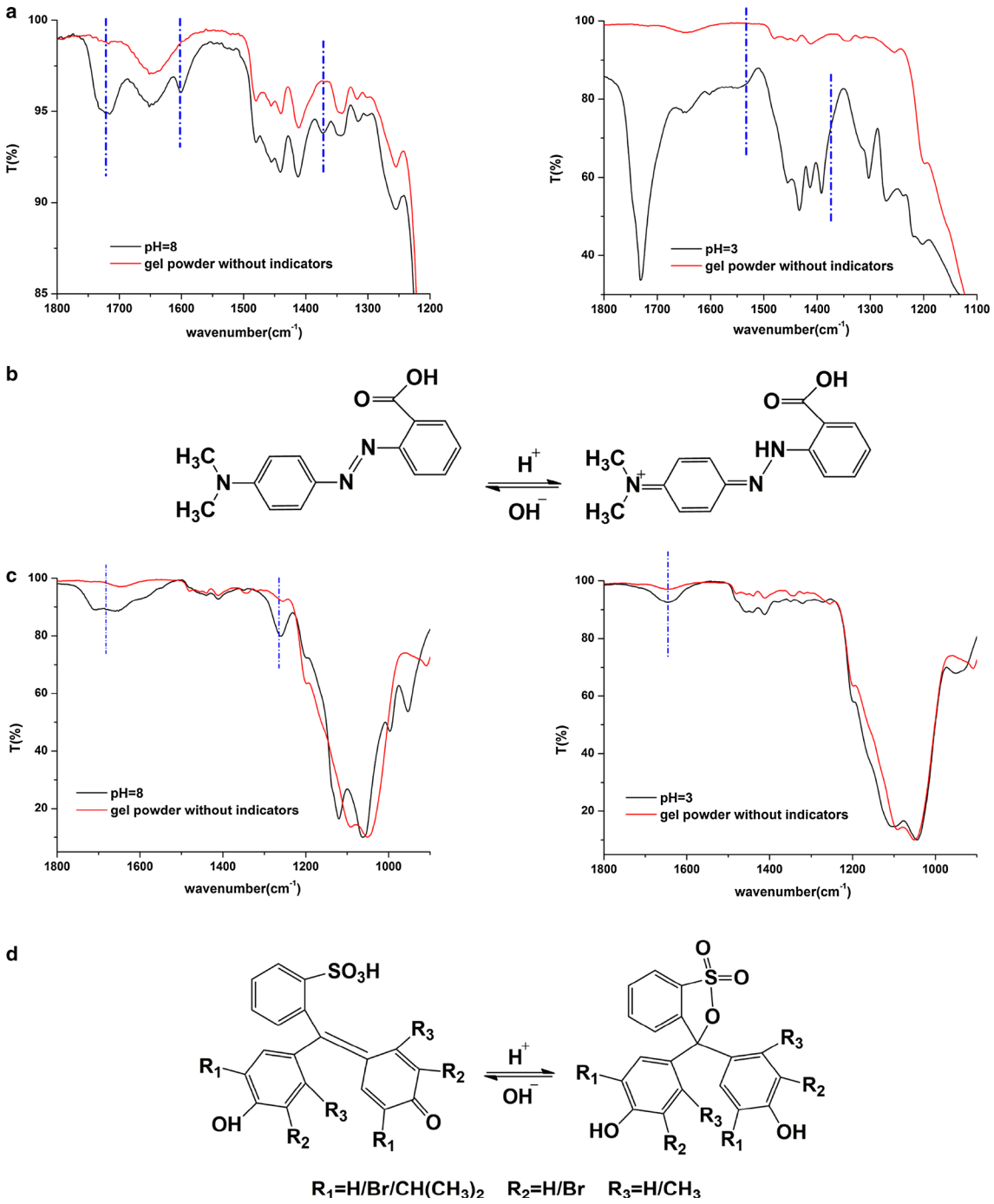

Fig. 4 FTIR spectra of **a** MR gel powder in different buffer, **b** tautomerism of MR molecule, **c** BCG gel powder in different buffer, **d** tautomerism of PR/BTB/BCG molecule

BCG gel powders in different buffers were conducted. Gel powders were placed in pH 3 or 8 buffers until the color change was complete. Compared with the pure gel powder, the spectrum of MR, pH 8 (Fig. 4a) has characteristic peaks resulting from C=O at 1,715 cm^{-1}, C=C at 1,600 cm^{-1} and stretching vibrations of N=N at 1,372 cm^{-1}. These represent the azo structure of MR under alkaline conditions. This peak disappeared upon protonation due to the presence of the hydrazone tautomer (Fig. 4b). The characteristic absorption of C=N at 1,550 cm^{-1} was not apparent in MR being encapsulated in the gel matrix. The BCG indicator presents a ring opening arising from the quinine (alkaline) to the lactone (acidic) form (Fig. 4d). The bands observed at 1,650–1,715 cm^{-1} and 1,260 cm^{-1} were attributed to the C=O vibrations and S=O stretching modes in the sulfonate moiety (Fig. 4c).

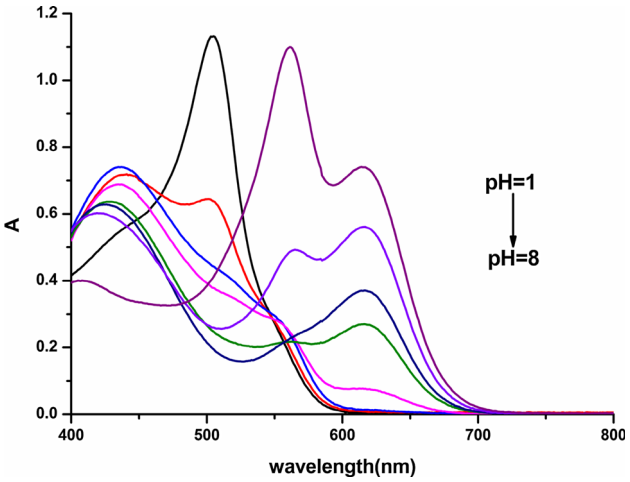

Fig. 5 Absorbance spectrum of sols solutions containing four indicators in different pH

The carbonyl peak still remains at pH 3 indicating a mixture of two tautomeric forms due to constraining factors by the gel and the larger molecular volume of BCG. Stretching vibrations of the benzene ring and S=O stretching in lactone were overlapped by Si–O–Si and C–O–C of gel from 1,000 to 1,200 cm^{-1}.

The absorptions spectrum of sol solutions is shown (Fig. 5). It is worth noting that the halochromic behavior of dyes in a sol–gel cotton matrix differed from the sol-solution systems. There was a different color in the range pH equals 7–8. This could be attributed to the interactions of indicator molecules with their surrounding environment. The dyes in cotton samples were mainly located in the silica substrate, which appears to produce a different interaction with the guest molecules through the polarization effect compared to that in water [29, 30]. Thus, different transition energy of $n \rightarrow \pi^*$ obtained from the effect brought out different colors. Another reason was that the partially hydrophobic silica gel didn't completely cover the cotton fabric, only the indicators situated on the surface layer of gel could be protonated by H^+, which was conveyed by the water or the water in the holes of cotton. So the color was a mixture of protonated indicators and unprotonated ones.

The dynamic behavior of the pH response was conducted by placing finished samples in the different buffers and then in deionized water (pH = 6.56) to recover the color. The process was repeated ten times and the color variation (ΔE) and La*b* was quantified in Tables 1 and 2 to determine the behavior to pH response.

It should be noted that a similar trend was evident from the hue of the samples in terms of varying process times where a* continues to rise and b* initially increases and then falls back (Table 1). Due to the elution of indicators not encapsulated, a general drop in color variation was evident with increase of processing times apart from the pH 3 and 5 samples where a larger ΔE was determined (Table 2). This could occur due to the polarity of the silicon gel that differs from cotton, in which the indicator develops a more prominent color. A minimum of 5.69 between pH 2 and 3 in the sample processed ten times suggested that color differences could be distinguished by naked eyes [29]. When immersed in deionized water, the sample color-recovering time (pH5–8) increased from 1 to 5 min along with the processing times, while the pH1–4 samples took longer for proton exchange to occur. When immersed in buffers each sample completely change its color in 30 s even after the 10th process. If the finished cotton was firstly immersed in water for 24 h to clear up the non-encapsulated indicators, the ΔE of different process times was close to zero and the color-changing time of each pH value accordingly increased to about 10 min owing to a slower permeation of water into the interior of the finished cotton to protonate indicators.

Table 1 La*b* value for each pH in finished cotton processed 0, 5 and 10 times

	L	a*	b*
Processed 0 times			
pH 1	58.57	45.09	17.93
pH 2	62.95	26.12	31.89
pH 3	61.79	31.16	30.51
pH 4	63.85	25.21	33.02
pH 5	62.71	15.61	31.67
pH 6	61.55	2.98	25.66
pH 7	61.94	−6.94	23.84
pH 8	57.07	−8.76	11.32
Processed 5 times			
pH 1	64.77	35.18	18.96
pH 2	66.5	27.73	25.86
pH 3	68.58	22.66	26.51
pH 4	68.05	15.9	27.58
pH 5	73.2	−4.62	30.29
pH 6	72.22	−5.97	26.05
pH 7	67.04	−12.77	19.07
pH 8	66.44	−11.44	7.05
Processed 10 times			
pH 1	69.37	28.05	27.27
pH 2	72.27	17.82	29.94
pH 3	73.36	17.16	24.39
pH 4	72.39	10.93	31.34
pH 5	74.95	−4.86	31.96
pH 6	75.03	−7.72	27.02
pH 7	72	−10.72	20.7
pH 8	68.94	−11.22	14.65

Table 2 ΔE for each pH in cotton processed 0, 5 and 10 times

	pH 2	pH 3	pH 4	pH 5	pH 6	pH 7	pH 8
Processed 0 times							
pH 1	23.96	19.04	25.51	32.79	42.92	52.47	54.27
pH 2		5.35	1.71	10.52	24.00	34.04	40.92
pH 3			6.78	15.62	28.60	38.68	44.54
pH 4				9.76	23.53	33.49	40.88
pH 5					14.04	22.88	32.25
pH 6						10.09	19.07
pH 7							13.56
Processed 5 times							
pH 1	10.30	15.11	21.37	42.23	42.42	48.00	48.15
pH 2		5.52	12.05	33.33	34.18	41.07	43.45
pH 3			9.38	27.93	28.86	36.24	39.32
pH 4				21.33	22.32	29.92	34.23
pH 5					4.56	15.17	25.15
pH 6						11.04	20.60
pH 7							12.11
Processed 10 times							
pH 1	10.96	11.95	17.85	33.71	36.22	39.41	41.25
pH 2		5.69	7.03	22.93	25.85	30.00	32.99
pH 3			6.86	23.34	25.07	28.16	30.33
pH 4				16.01	19.32	24.13	27.95
pH 5					5.71	13.03	19.40
pH 6						7.63	14.23
pH 7							6.80

3.3 Interaction between indicators and gel matrix

Interaction between indicators and gel matrix was characterized by ^{29}Si NMR spectra of gel powders added with MR (Fig. 6, 1-a and BCG (Fig. 6, 2-a), which were cured at 120 °C for 1 h. From high field to low field, there existed characteristic peaks at −57.85 ppm corresponding to the T_2 structure (two of the three silinol were condensed), −65.62 ppm to T_3, −92.40 ppm to Q_2, −102.04 ppm to Q_3 and −110.61 ppm to Q_4 in Fig. 7. The un-condensed structures T_0, Q_0 and T_1 were not produced. When MR added, the proportion of T_3 and Q_4 increased while the others decreased, which suggested that hydrolysis and condensation of precursors had raised. Because the –Si–O–Si– structure was mainly formed during the drying and curing process and MR indicators did not have great influence in this process due to small size of MR molecules. Moreover, MR was positively charged in the acidic preparation conditions and could bridge silanol molecules to increase the level of condensation. The BCG molecule is twice bigger than the MR and could not be protonated in acid so that it has an adverse effect on the condensation. Thus the amount of Q_3 was larger than Q_4.

3.4 Characterization of gel material

The ^{13}C NMR spectra of TEOS and GPTMS precursors are shown in Fig. 8. TEOS exhibit signals at δ 17.91(Cb) and δ 58.96(Ca). GPTMS shows signals at δ 73.23(Cc), δ 71.22(Cd), δ 50.61(Ce), δ 50.23(Cf), δ 43.91(Cg), δ 22.96(Ch) and δ 5.06(Ci) [31].

Solid state ^{13}C NMR spectra of gel materials prepared in different conditions are presented in Fig. 9a. The characteristic peaks, 9.11 and 22.67 ppm, correspond to the $–CH_2–CH_2–$ structure in GPTMS. The signals for the epoxy group, δ 44.51(Cg) and δ 51.43(Cf), have significantly reduced after curing, which suggests that temperature treatment contributed to the opening of epoxy group and several possible reaction paths are illustrated in Fig. 9b. The disappearance of signals for TEOS and OMe of GPTMS indicated that a complete hydrolysis and a consequent condensation had taken place. The new peak, 63.9 ppm corresponding to the hydroxyl carbon of diols in path 2 shows a dramatic decrease in sample b. This phenomenon implies that the curing process is conducive to the inhibition of the formation of diols which could stop the polymerization in GPTMS. The sharpening of the peaks from 70 to 75 ppm in the gel being cured implies that the presence of shorter poly (ethylene oxide) chain derivative [32]. Furthermore, the reaction between the epoxy group

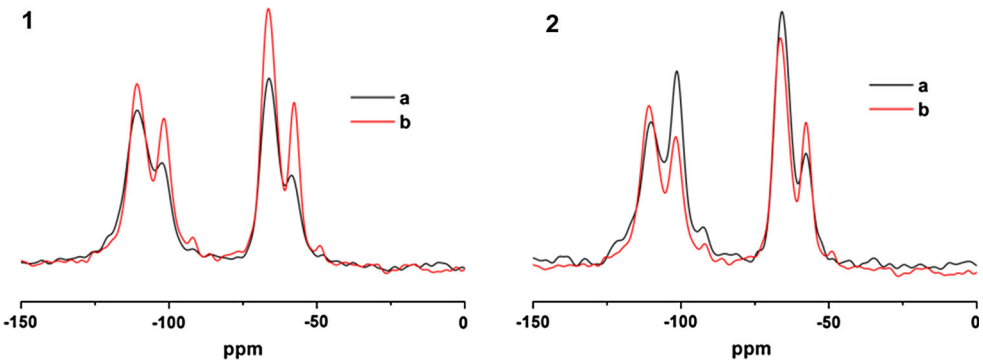

Fig. 6 ^{29}Si NMR spectra of gel: **1**-*a* gel containing MR, **1**-*b* pure gel, **2**-*a* gel containing BCG, **2**-*b* pure gel

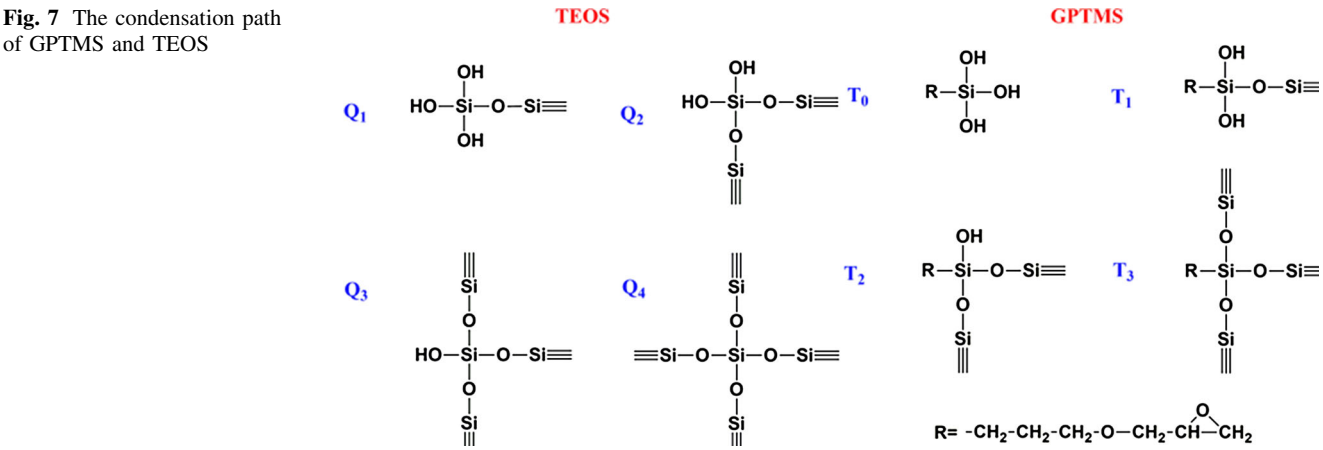

Fig. 7 The condensation path of GPTMS and TEOS

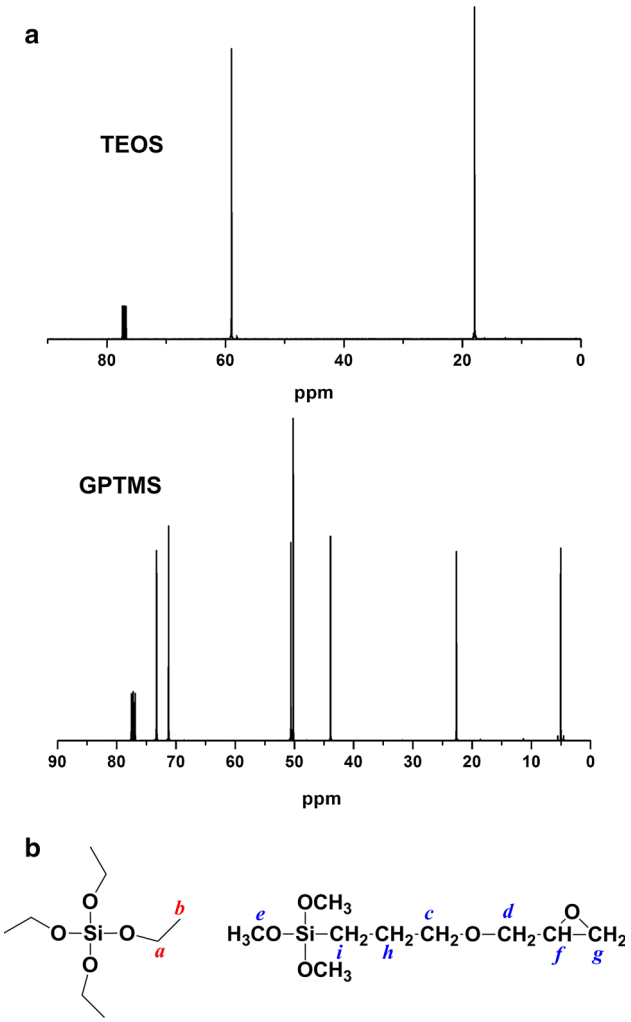

Fig. 8 **a** ^{13}C NMR spectra and **b** chemical structures of TEOS and GPTMS

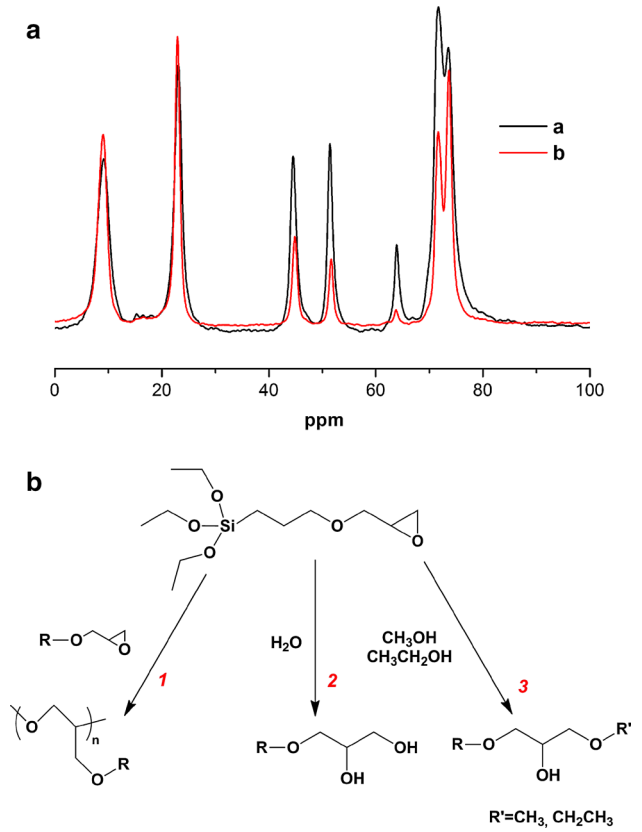

Fig. 9 **a** Solid state ^{13}C NMR spectra of gel powders containing no indicators (*a*) with curing or (*b*) without curing and **b** its possible reaction path

and alcohol in path 3 was not observed. These results suggest that the organic–inorganic hybrid structure was formed during curing which plays a key role in retaining indicators against leaching.

3.5 Leaching activity

The K/S ratio of the fabric samples can be used as a semi-quantitative method to display the amount of dyes in fabrics, and the sum of K/S value from 400 to 700 nm was employed to represent the ability against leaching(CY = Color Yield), with n being 24 or 48 h (Fig. 10).

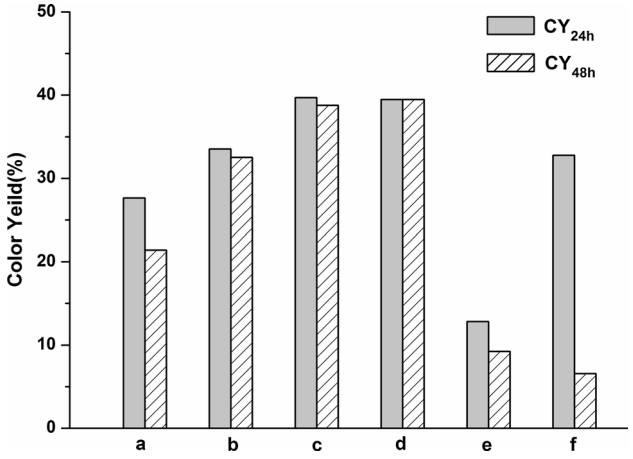

Fig. 10 Leaking activity of *a* sol–gel finished cotton with MR, *b* sol–gel finished cotton with PR, *c* sol–gel finished cotton with BTB, *d* sol–gel finished cotton with BCG, *e* sol–gel finished cotton with BCG (TEOS only), *f* conventional dyeing cotton with BCG

$$\mathrm{CY_n}(\%) = \frac{(\mathrm{K/S})_\mathrm{n}}{(\mathrm{K/S})_0} \times 100\%.$$

Before testing, MR treated-fabric was immersed in pH 3 until color change had taken place, similarly the BCG and PR were treated in pH 8 and BTB in pH 9 buffers.

We observed a significant drop in the K/S value for all fabrics when soaked for 24 h which means that some indicators were not completely encapsulated in the gel matrix and released into the medium. Due to the uneven distribution of sol solutions on fabric gel coating is unable to form a consistent structure. Thus, the internal tension resulting from the condensation and evaporation of solvent during curing give rise to the cracks formation (Fig. 1), especially for the surface in textiles [33]. Moreover due to a lack of strong interactions, indicators located in the cracks and on the coating surface diffused into water after the first 24 h treatment.

The fabrics appear to have different leaking characteristics when exposed to the second immersing phase (24–48 h). The K/S values of BCG, BTB and PR are barely unaltered which suggests no leaking occurs for the three indicators in this stage of the process however but some leakage takes place for MR. In contrast to MR, there are three benzene rings in the molecular structure of BCG, BTB and PR so that the higher molecular weight and planarity factors contribute to enhancing the affinity within the silica matrix. On the other hand, the silica coating exhibits a negative charge in water (pH = 6.5–7) since its isoelectric point is around pH 4 [34]. Overall MR is negatively charged by ionization of the carboxyl group thus larger repulsion forces are present between MR and the substrate.

Table 3 Tensile strength (warp direction)

	Breaking force F (N)	Breaking L (mm)	Elongation E (%)
1	727.5	17.69	17.69
2	198	11.94	11.94
3	650.5	17.06	17.06
4	570.5	15.06	15.06

1, untreated cotton; 2, conventional dyeing cotton with BCG; 3 sol–gel finished cotton without indicators; 4, sol–gel finished fabric with four indicators

The different dyeing systems were compared, sample d, e and f being considered. TEOS was the only sample yielding less color compared to the mixed sol system. This suggests that the organic net structure formed by GPTMS, as illustrated by ^{13}C NMR (Fig. 9) prevents leakage. In conventional dyeing processes, there was no probability of cross linking between the dye and the fabric. Hence diffusion effects generated by concentration gradients lead to leakage and loss of dye.

3.6 Tensile strength

Since the fabric tensile properties can be greatly affected by the sol–gel treated process, tensile test of the warp was conducted (Table 3). The conventional sample demonstrated the greatest fall in breaking force and elongation. This being due to the large degradation of cellulose glycosidic bonds under acid conditions and high-heat flux. Treated by the pure sol solutions, the dense gel film formed by hydrolysis and condensation on the fabric gave rise to an enhanced increase in the tensile strength, but this remains inferior to the untreated cotton. The tensile strength fell further with the addition of indicators due to the dye influencing the integrity and continuity of the film (Fig. 1).

4 Conclusion

In summary, we have shown that universal halochromic textiles were successfully prepared by incorporating a combination of pH indicators into a gel network. Interaction between indicators and silica matrix gave rise to a color-changing film being formed on cotton, and different halochromic behavior was exhibited compared to the sol solution. The finished cotton displayed a noticeable differences in ΔE between each pH. Indicators with high weight and less negative charge were stable, while a lack of affinity leads to leakage. The epoxy ring opening in GPTMS precursors was observed and the organic cross-linking coupled with the inorganic condensation validated the capsulation of pH indicators. The charge and size of

indicators played key roles in the interaction between the gel matrix and guest molecules. The gel coating could support the tensile strength properties of cotton, which was damaged by acid and heat treatments. It is viewed that the halochromic textile could be developed as a tool for pH sensing and expanding the application of pH concentration measurements in fabrics.

Acknowledgments This work was financially supported by the UK–China Joint Laboratory for Therapeutic Textiles (based at Donghua University), and the Biomedical Textile Materials "111 Project" of the Ministry of Education of P.R. China (B07024).

References

1. Carmona N, Bouzas V, Jimenez F, Plaza M, Perez L, Garcia MA, Villegas MA, Llopis J (2010) Sens Actuators B-Chem 145:139–145
2. Brancatelli G, Colleoni C, Massafra MR, Rosace G (2011) Polym Degrad Stab 96:483–490
3. Xu FG, Yu JG, Li D, Xiang N, Zhang QJ, Shao L (2014) J Sol–Gel Sci Technol 71:204–210
4. Zhang HZ, Wang XD, Wu DZ (2010) J Colloid Interface Sci 343:246–255
5. Albarran L, Lopez T, Quintana P, Chagoya V (2011) Colloid Surf A 384:131–136
6. Dickson DJ, Ely RL (2013) Appl Microbiol Biotechnol 97:1809–1819
7. Cui LR, Lin HM, Guo W, Xiang D, Zhou D, Zhang T, Qu FY (2014) J Sol–Gel Sci Technol 72:106–113
8. Jeronimo PCA, Araujo AN, Montenegro MCBSM (2007) Talanta 72:13–27
9. Walcarius A, Collinson MM (2009) Annu Rev Anal Chem 2:121–143
10. Buntem R, Intasiri A, Lueangchaichaweng W (2010) J Colloid Interface Sci 347:8–14
11. Capeletti LB, Bertotto FL, Dos Santos JHZ, Moncada E, Cardoso MB (2010) Sens Acutators B-Chem 151:169–176
12. Capeletti LB, Radtke C, Dos Santos JHZ, Moncada E, da Rocha ZN, Pepe IM (2011) Colloid Surf A 392:256–263
13. Ismail F, Schoenleber M, Mansour R, Bastani B, Fielden P, Goddard NJ (2011) Analyst 136:807–815
14. Schramm C, Binder WH, Tessadri R (2004) J Sol–Gel Sci Technol 29:155–165
15. Mahltig B, Fiedler D, Fischer A, Simon P (2010) J Sol–Gel Sci Technol 55:269–277
16. Mahltig B, Fischer A (2010) J Polym Sci Polym Phys 48:1562–1568
17. Textor T, Mahltig B (2010) Appl Surf Sci 256:1668–1674
18. Yin YJ, Wang CX, Wang CY (2008) J Sol–Gel Sci Technol 48:308–314
19. Zimehl R, Textor T, Bahners T, Schollmeyer E (2004) Prog Colloid Polym Sci S 125:49–53
20. Wang RH, Wang XW, Xin JH (2010) Acs Appl Mater Interfaces 2:82–85
21. Christie RM, Bryant ID (2005) Color Technol 21:187–192
22. Little AF, Christie RM (2010) Color Technol 126:157–163
23. Osti E (2008) Ann Burns Fire Disasters 21:73–77
24. Van Geluwe S, Braeken L, Van der Bruggen B (2011) Water Res 45:3551–3570
25. Van der Schueren L, De Clerck K (2012) Color Technol 128:82–90
26. Van der Schueren L, De Clerck K, Brancatelli G, Rosace G, Van Damme E, De Vos W (2012) Sens Acutators B-Chem 162:27–34
27. Jurmanovic S, Kordic S, Steinberg MD, Steinberg IM (2010) Thin Solid Films 518:2234–2240
28. Nielsen SS (2003) Study Questions Ultraviolet, Visible, and Fluorescence Spectroscopy. In: Nielsen SS (ed) Instructor's manual for food analysis. Springer, US, pp 111–114
29. Wang LQ, Peng XJ, Song FL, Lu E, Cui JN, Gao XQ, Lu RW (2004) Dyes Pigm 61:103–107
30. Trupp S, Alberti M, Carofiglio T, Lubian E, Lehmann H, Heuermann R, Yacoub-George E, Bock K, Mohr GJ (2010) Sens Acutators B-Chem 150:206–210
31. Innocenzi P, Brusatin G, Guglielmi M, Bertani R (1999) Chem Mater 11:1672–1679
32. Innocenzi P, Brusatin G, Babonneau F (2000) Chem Mater 12:3726–3732
33. Kozuka H, Kajimura M, Hirano T, Katayama K (2000) J Sol–Gel Sci Technol 19:205–209
34. Panitz JC, Geiger F (1998) J Sol–Gel Sci Technol 13:473–477